Available online at www.sciencedirect.com
SCIENCE DIRECT®
Journal of Photochemistry and Photobiology A: Chemistry 171 (2005) 215–221
Journal of Photochemistry and Photobiology A:Chemistry
www.elsevier.com/locate/jphotochem

Aggregation and fast diffusion of dye molecules on air–glycerol interface observed by confocal fluorescence microscopy

Yoshihiro Takeda[a,*], Fumitaka Mafuné[b,1], Tamotsu Kondow[b]

[a] East Tokyo Laboratory, Genesis Research Institute Inc., 717-86 Futamata, Ichikawa, Chiba 272-0001, Japan
[b] Cluster Research Laboratory, Toyota Technological Institute, 717-86 Futamata, Ichikawa, Chiba 272-0001, Japan

Received 23 June 2004; received in revised form 15 October 2004; accepted 20 October 2004
Available online 8 December 2004

Abstract

Diffusion processes of Rhodamine 6G (Rh6G) dye molecules dissolved in a small hemisphere drop of glycerol on a cover glass were investigated by using a confocal fluorescence microscope equipped with an objective lens with a high numerical aperture (NA = 1.35). Photon burst signals from Rh6G molecules in the bulk glycerol and on the air–glycerol interface of the hemisphere drop were separately detected at a single molecule level. The analysis of the photon burst signals by a correlation function method reveals that a sizable portion of the Rh6G molecules in the drop are aggregated on the air–glycerol interface and diffuse two-dimensionally on it, while the rest diffuse molecularly in the bulk. The aggregates are found to have a diffusion constant 15 times as large as that of the Rh6G molecule in the bulk glycerol, although the aggregates have a hydrodynamical radius much larger than that of a Rh6G molecule.

Keywords: Rhodamine 6G; Air–glycerol interface; Single molecule detection; Confocal fluorescence microscopy; Diffusion constant; Aggregation

1. Introduction

Glycerol has been a subject of considerable and long-standing scientific interest. The presence of three hydroxyl groups makes glycerol a particularly complex system as hydrogen-bonded fluids. In bulk glycerol, each glycerol molecule is bound by hydrogen bonds, of which formation and disruption are responsible to the high-viscosity of glycerol [1,2]. On the other hand, the hydroxyl groups of glycerol molecules on a glycerol interface tend to orient inward, while the CH and the CH_2 groups stick out of the interface [3]. The hydroxyl groups on the interface give rise to a high surface tension of the glycerol [4]. These findings indicate that solute molecules on the interface of a glycerol solution should behave differently from those in the bulk, because the interface and the bulk give totally different environments on the solute molecules.

As for other liquids, extensive studies have also been undertaken to elucidate the fundamental properties of the interfaces by taking advantage of various surface-sensitive tools [5–7]. In any case, molecules targeted for the investigation are needed to be abundant enough to attain an acceptable signal-to-noise ratio. In dealing with a small number of solute molecules targeted for investigation in a solution, fluorescence microscopy facilitates detection of weak fluorescence signals from the target molecules through measuring bunching signals of the fluorescence instead of measuring integrated dc signals of the fluorescence, although fluorescence spectroscopy is not well-compatible with this methodology. In addition, the fluorescence microscopy with a confocal configuration is particularly suitable for the investigation of dynamical behaviors of individual fluorescing molecules in a solution [8–11].

It is favorable from an experimental viewpoint that the objective lens of a fluorescence microscope employed has a numerical aperture larger than ∼1.3 so as to collect a suffi-

* Corresponding author. Tel.: +81 47 320 5916; fax: +81 47 327 8030.
E-mail address: takeda@clusterlab.jp (Y. Takeda).
[1] Present address: Department of Basic Science, Graduate School of Arts and Sciences, The University of Tokyo, Komaba, Meguro-ku, Tokyo 153-8902, Japan.

1010-6030/$ – see front matter © 2004 Elsevier B.V. All rights reserved.
doi:10.1016/j.jphotochem.2004.10.014

cient number of fluorescence photons for the achievement of a single molecule detection. Note that the numerical aperture of the objective lens increases with the decrease of its focal length and hence the objective lens should have the shortest possible focal length. The sample and the micrometer should be so arranged that the objective lens is located at the closest possible distance to the sample.

In the present study, we prepared a hemispherical surface of a glycerol liquid containing a trace amount of Rhodamine 6G (Rh6G), which can be approached to the top of the objective lens at the distance of several tens micrometer, and investigated diffusion of a single Rh6G molecule in a bulk glycerol and its aggregate on an air–glycerol interface by using a confocal fluorescence microscope equipped with an objective lens of a large numerical aperture (NA = 1.35). In practice, the air–glycerol interface of the hemisphere drop of the Rh6G-containing glycerol solution on a cover glass was placed at a distance of several tens micrometer from the top of the objective lens by taking advantage of the fact that glycerol has a high surface tension. Bunching signals of fluorescence from Rh6G were measured by changing the position of the objective lens, with adjusting the focal point of an excitation laser either on the air–glycerol interface or the inside of the hemisphere drop.

2. Experimental

2.1. Materials and sample preparation

At first, a concentrated Rh6G solution in glycerol was prepared. Then, a working solution was prepared by serially diluting the solution with glycerol down to 2.5 nM, and was stored in a glass vial wrapped in an aluminum foil for prevention from photo-degradation. Commercially available glycerol (Kanto Chemical Co. Inc.) and Rh6G (Eastman Kodak Co. Inc.) were used without further purification.

2.2. Apparatus

The confocal fluorescence microscope system used consists of an inverted microscope (IX70, Olympus Inc.), a CW argon ion laser (177G, Spectra-Physics) for the excitation of Rh6G, and a silicon avalanche photodiode (Model SPCM, EG&G Canada, a quantum efficiency of ∼75% and a dark noise of ∼7 counts/s) as the detector of fluorescence. The inverted microscope is equipped with an oil immersion objective lens having a numerical aperture of 1.35 (UplanApo 100×). The argon ion laser was introduced into the objective lens after being reflected by a dichroic beam-splitter and was tightly focused onto a sample solution. Under irradiation of the argon ion laser at 488 nm, a Rh6G molecule in the focusing region (designated as focal region or focal volume) of the objective lens, in which the excitation laser is the most tightly focused, emits 10^6 to 10^8 photons/s by repeating absorption and emission cycles. The fluorescence photons were collected by the same objective lens for the detection by the silicon avalanche photodiode. In the present confocal system, photons coming from the outside of the focal volume were removed by a pinhole (50 μm in diameter) placed on the primary image plane. The dichroic beam-splitter and a single interference bandpass filter (BP545-580, Omega Optical Inc.) were used to remove the excitation laser light and the Rayleigh- and Raman-scattered light. Both the pinhole and the silicon avalanche photodiode detector were mounted on *xyz* transition stages for precise alignment. Photon signals were acquired by using a multichannel scalar (SR430, Stanford Research System) based on a personal computer.

2.3. Measurement

A 100 μL sample solution was dropped on a cover glass, and was wiped back and forth until it became hemisphere drops with diameters of several tens micrometers. The cover glass was approached to the objective lens as closely as possible. At the first place, the excitation laser beam was focused above the air–glycerol interface of a hemisphere drop, namely, the focal volume is located just above the interface of the drop. Then, the focal volume was lowered by ∼1 μm with moving the objective lens downward, and the fluorescence signals were measured. The same measurement was repeated by lowering the focal volume by another ∼1 μm and so on, so that the most appropriate location was discovered for collecting the fluorescence signals from a desired place (air–glycerol interface, inside, etc.) of the drop (see Fig. 1). The fluorescence was detected and counted with the gate time of 1.31 ms. One peaked signal collected in the gate time of 1.31 ms is designated as ‘fluorescence photon count’ whose height is measured as counts per 1.31 ms, while a bunch of fluorescence photon counts resulting from a fluorescing species (a single Rh6G molecule or its aggregate) traversing across the focal volume is designated as ‘photon burst’ consisting of a finite number of fluorescence photon counts varying with the trajectories of the fluorescing species together with the spatial intensity distribution of the excitation laser beam.

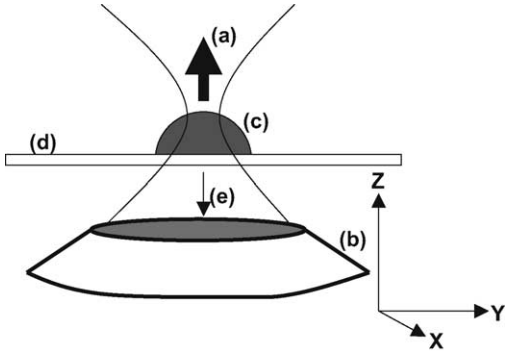

Fig. 1. Schematic diagram in the vicinity of the probe region of the apparatus employed: (a) excitation laser, (b) objective lens, (c) hemisphere drop of glycerol, (d) cover glass and (e) fluorescence.

A hemisphere drop with ∼25 μm in radius can be treated as having a flat surface inside the focal volume, because the excitation laser is tightly focused in a ∼1 μm^2 spot, where the difference in height between the center and the brim of the cross-sectional area of the focal volume on the interface is as large as 10^{-14} m [12]. All the measurements were conducted at the temperature of 307 K.

3. Results

3.1. Time evolutions of fluorescence photon counts

Fig. 2(a and b) shows time evolutions of fluorescence photon counts when the excitation laser beam is focused by the objective lens on the air–glycerol interface of a hemisphere drop of glycerol (defined as the depth of 0 μm) and at the depth of 14.9 μm inside the drop from the interface (defined as the depth of 14.9 μm). Each arrow in Fig. 2b indicates a photon burst signal generated from a single Rh6G molecule traversing through the focal region. As shown in Fig. 2b, the signal-to-noise ratios for the photon bursts detected at the depth of 14.9 μm (inside the glycerol hemisphere drop) were not satisfactorily high, although the instruments are so arranged deliberately in the present measurement system that Rayleigh-scattering light of the excitation laser intensified due to the high-refractive index of glycerol is attempted to be minimized by minimizing the thickness of the glycerol solution between the focal region and the top of the objective lens. The widths and the intensities of the photon bursts detected at the air–glycerol interface (see Fig. 2a) differ significantly from those detected at 14.9 μm deep inside the drop (see Fig. 2b).

3.2. Height distribution of fluorescence photon counts

Fig. 3 shows a typical histogramic height distribution (solid bars) of the fluorescence photon counts observed in the photon bursts (derived from Fig. 2a) when the focal volume is located on the air–glycerol interface of the hemisphere drop, and that (striped bars) (derived from Fig. 2b) when the focal volume is inside it; the abscissa and the ordinate represent the height and the frequency of the fluorescence photon counts, respectively. A photon burst is observed when a single fluorescing particle (Rh6G molecule or its aggregate) in a Brownian motion is traversing the focal volume. Therefore, the height distributions carry information on both the fluorescence intensity and the trajectories of the fluorescing particle together with the spatial intensity distribution of the excitation laser beam.

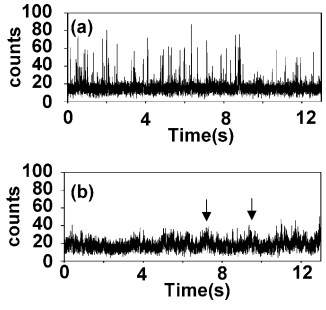

Fig. 2. The fluorescence photon bursts consisting of low and high fluorescence photon counts of Rh6G at the depths of (a) 0 μm and (b) 14.9 μm measured from the air–glycerol interface of a hemisphere drop of glycerol containing a trace amount of Rh6G dye. The arrow indicates the photon burst signal generated from a single Rh6G molecule.

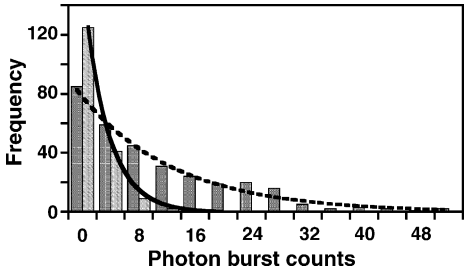

Fig. 3. The histogram given by solid bars represent the height distribution of the fluorescence photon counts in the high photon bursts (consisting of fluorescence photon counts higher than 40 counts/1.31 ms), which are obtained by extracting them from the time evolution measured at the depth of 0 μm. The histogram given by striped bars represent the height distribution of the fluorescence photon counts, which is obtained from the time evolution measured at the depth of 14.9 μm. Solid and dotted lines represent the fitting exponential functions to the histograms.

3.3. Correlation analysis

The average width of photon bursts observed during a time-evolution measurement was estimated by using a correlation analysis. Fig. 4 shows the autocorrelation of the photon bursts calculated from the time evolution shown in Fig. 2b. The correlation analysis relates the number of the fluorescence photon counts $C(t)$, at time t, with those, $C(t+\tau)$, at time $t+\tau$. By integrating the product, $C(t)C(t+\tau)$, over a measurement time period, T_m, on the premise that a sufficiently large number of photon bursts are acquired, the autocorrelation function $G(\tau)$ [13] is obtained as

$$G(\tau) = \int_0^{T_m} C(t)\, C(t+\tau)\, dt \quad (1)$$

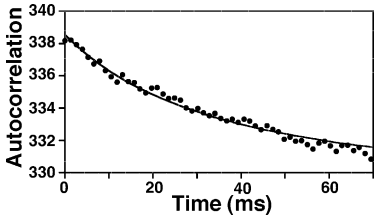

Fig. 4. The autocorrelation of the photon burst signals calculated from the time evolution shown in Fig. 2b.

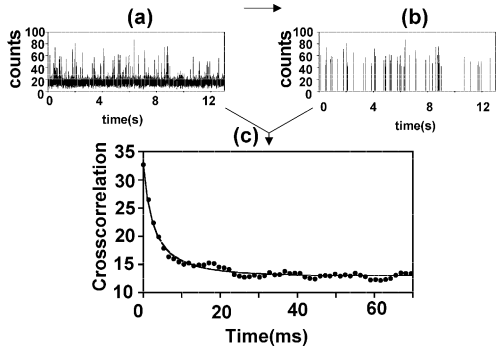

Fig. 5. The time evolution measured at the depth of 0 μm (a) is used to derive the time evolution of the fluorescence photon counts higher than 40 counts/1.31 ms (b). (c) The cross correlation function in the fluorescence photon counts in the high photon bursts thus obtained is shown.

where $G(\tau)$ is not normalized over the measurement time period, T_m. As shown in Fig. 4, $G(\tau)$ which is the largest at $\tau = 0$ decreases monotonically with time τ.

Photon bursts observed at the depth of 0 μm (the air–glycerol interface) contain both fluorescence signals from the air–glycerol interface and the bulk glycerol (Fig. 2a), because a spatial resolution (about 1 μm) in the direction of z-axis is insufficient to discriminate the contribution of the bulk. In order to characterize a diffusion process of a fluorescing particle on the air–glycerol interface, the width of the photon bursts assignable to the interface was estimated by a cross-correlation analysis. Firstly, the time evolution of the fluorescence photon counts purely from the air–glycerol interface was obtained by extraction of the fluorescence photon counts higher than 40 counts/1.31 ms from the time evolution measured at the depth of 0 μm (on the air–glycerol interface) (see Fig. 2a); as shown later, the fluorescence photon counts higher than 40 are considered to be generated from fluorescing particles on the interface. Secondly, the time evolution thus obtained was cross-correlated with the time evolution measured at the depth of 0 μm. The cross-correlation function (see Fig. 5) thus obtained is related to the fluorescence photon counts purely from the air–glycerol interface.

4. Discussion

4.1. Intensity of fluorescence photon bursts and aggregation of Rh6G on air–glycerol interface

As described above, a photon burst consisting of weak fluorescence photon counts is observed when one Rh6G molecule traverses the focal volume in the bulk glycerol (see Fig. 2b), while a photon burst consisting of strong fluorescence photon counts is observed when an aggregate of Rh6G molecules traverses, as observed on the air–glycerol interface (see Fig. 2a). In order to substantiate the above statement, we derive information on the average intensity of fluorescence being emitted by a Rh6G molecule and that by a Rh6G aggregate, by analyzing the height distributions (solid and striped bars of Fig. 3) of fluorescence photon counts from the interface and the bulk; the frequency of the fluorescence photon counts having a height of x_i (count per 1.13 ms) is given by $h(x_i)$. This function has such a character that even if the concentration and the excitation rate of a fluorescing particle are increased by n times, the same functional form is obtained by elongating y-axis (the frequency of the fluorescence photon counts) and x-axis (the height of the fluorescence photon counts) by n times, respectively. Assuming that $h(x)$ for a given fluorescing particle is reproduced reasonably well by a statistical distribution function, $f(x)$, a height distribution of fluorescence photon counts given by a different particle fluorescing n times as many photons as the former one under the same measurement condition is reproduced by a function $f(x/n)$. Namely, with increasing the fluorescence intensity by n times, x-axis representing the height of the fluorescence photon counts should be elongated by n times.

For simplification of the mathematical treatments, an exponential function $A\exp(-\lambda x)$ is introduced as the fitted distribution function $f(x)$. Comparing the functions $f(x/n)$ with $A\exp(-\lambda x)$, one obtains that the exponent, λ, is proportional to $1/n$ ($\lambda \propto 1/n$). The validity of using the exponential function, $A\exp(-\lambda x)$, as the fitting function to $h(x)$ was confirmed by 'χ^2-test of goodness-of-fit-method' [14,15]. Utility of the exponential function enables us to remove the uncertainty introduced from the background noise (Po) as follows: substituting x with $x - \mathrm{Po}$, in $f(x)$, one obtains

$$f(x) = A\exp(-\lambda(x - \mathrm{Po})) = A\exp(\lambda \mathrm{Po})\exp(-\lambda x) = A'\exp(-\lambda x) \quad (2)$$

The exponents (λ_s and λ_b) of $f(x)$ obtained from the height distributions of fluorescence photon counts related to the air–glycerol interface and the bulk were obtained to be 0.07 and 0.34, respectively. By using the relation, $\lambda \propto 1/n$, the intensity ratio, I_s/I_b, turns out to be $\lambda_b/\lambda_s = 4.5$, where I_s and I_b represent the average fluorescence intensities of the fluorescence photon counts from the air–glycerol interface and the bulk, respectively.

As shown in Figs. 2b and 3, fluorescence photon counts collected from the bulk glycerol in which Rh6G molecules are dissolved homogeneously and separately, are found to be smaller than 40 counts/1.31 ms), while as shown in Fig. 2a, fluorescence photon counts higher than 40 are the most abundant in probing the fluorescence collected from the air–glycerol interface. Much higher fluorescence photon counts in probing the air–glycerol interface than those in the bulk glycerol lead us to conclude that Rh6G molecules are aggregated on the interfaces and fluorescence photon counts higher than 40 are generated mostly from a single aggregate traversing through the focal volume located in the vicinity of the interface.

Let us estimate the size of the aggregate of a Rh6G on the air–glycerol interface. Under irradiation of the 488 nm laser on the air–glycerol interface of a hemisphere drop of glycerol

containing Rh6G, the fluorescence intensity of a Rh6G aggregate per constituent Rh6G molecule is apparently changed by: (1) reduction of the quantum-efficiency per Rh6G molecule due to non-fluorescent quenching of excite states of the aggregate [16–20], (2) change of the absorption cross-section per Rh6G molecule due to a blue shift of the corresponding absorption peak of the aggregate on the interface in comparison with that of a Rh6G molecule dissolved homogeneously and separately in the bulk glycerol, and (3) change of the fluorescence wavelength of the Rh6G aggregate due to a red shift of the fluorescence wavelength in comparison with that of a Rh6G molecule dissolved homogeneously and separately in the bulk glycerol. The change of the fluorescence intensity is estimated as follows: (1) the ratio of the quantum-efficiency of the Rh6G aggregate to that of the Rh6G molecule is reduced to 0.02 [16–20], (2) the excitation efficiency of the Rh6G aggregate is 1.5 times as large as that of the Rh6G molecule, and (3) the detection efficiency of the fluorescence of the Rh6G aggregate on the interface is reduced to ∼0.2 times as large as that in the bulk. By taking these into consideration, the fluorescence intensity per constituent Rh6G molecule from the Rh6G aggregate on the air–glycerol interface amounts to $\sim 6.0 \times 10^{-3}$ ($= 0.02 \times \sim 1.5 \times \sim 0.2$) of the fluorescence intensity of the Rh6G molecule. The average size of the Rh6G aggregate formed on the air–glycerol interface is given by the fluorescence-intensity ratio ($I_s/I_b = 4.5$) divided by the fluorescence-intensity change ($\sim 2.4 \times 10^{-3}$); the average size turns out to be $4.5/6.0 \times 10^{-3} \sim 7.5 \times 10^2$.

The number density of Rh6G molecules on the air–glycerol interface increases up to $\sim 10^5$ molecules/m^2, which is calculated by using the results that high photon bursts (consisting of fluorescence photon counts higher than 40 counts/1.31 ms) of Rh6G aggregates are observed at a rate of ∼14 counts/s and the radius of the hemisphere drop is ∼25 μm. In return, the Rh6G concentration inside the hemisphere drop decreases down to ∼0.1 nM from the concentration (2.5 nM) of a freshly prepared solution, since almost all the Rh6G molecules are condensed as aggregates on the air–glycerol interface as described above. In this concentration, the probability of finding one Rh6G molecule in the probe volume (focal volume) is 0.09 so that Rh6G molecules inside the hemisphere drop should be detected at a single molecule; actually low photon bursts (consisting of fluorescence photon counts lower than 40 counts/1.31 ms) were observed when the probe volume was located inside it. Unless otherwise, the probability of finding one Rh6G molecule in the probe volume should increases up to 0.62 and the photon signals should be semi-continuous.

4.2. Diffusion of Rh6G in bulk glycerol

The average width of photon bursts is obtained from the correlation analysis of the photon bursts; the width is related to the average transit time (across the probe volume) of individual Rh6G molecules or aggregates emitting the photon bursts. The average transit time also relates to the hydrodynamic radius of a Rh6G molecule or an aggregate of it and the viscosity of glycerol.

Fig. 4 shows the autocorrelation function calculated for Rh6G molecules in a bulk glycerol. The translational correlation function for a Rh6G molecule, which has three translational degrees of freedom, entering and leaving the probe volume is given theoretically as in Refs. [21,22]

$$G(\tau) = G_b(0)\left(1 + \frac{\tau}{\tau_{D_b}}\right)^{-1}\left(1 + \frac{\tau}{q^2\tau_{D_b}}\right)^{-1/2} + \text{Const.} \tag{3}$$

where q is ω_z/ω_{xy}, and ω_z and ω_{xy} are the $1/e^2$ probe depth (z) and the $1/e^2$ radius at the focal plane, respectively, in the confocal microscope. The parameter, $G_b(0)$, is the second power of the intensity of fluorescence from the Rh6G molecule in the bulk and τ_{D_b} is the diffusion time of the Rh6G molecule across the probe volume. For a propagating Gaussian laser beam focused by an objective lens, ω_{xy} is given by $\lambda f/n\pi d_0$, where λ is the laser wavelength in the vacuum, f the focal length of the objective lens, n the refractive index of the media ($n = 1.52$ for immersion oil) and d_0 the radius of the laser beam. The $1/e^2$ radius at the focal plane is calculated to be 450 nm under the present experimental condition. In principle, the $1/e^2$ probe depth (z) in confocal microscopy is derived from a point-spread function and a collection-efficiency function. In practice, however, the depth is primarily determined by the spherical aberration of the objective lens, and is given to be $\omega_z = 1.0$ μm [12]. The probe volume with a cylindrical symmetry amounts to 0.64 fL. Using a nonlinear least square minimization routine for fitting Eq. (3) to the autocorrelation shown in Fig. 4, one obtains the average transit time of $\tau_{D_b} = 47.9$ ms. As the average transit time τ_D is related to the diffusion constant D as

$$D = \frac{\omega_{xy}^2}{\tau_D} \tag{4}$$

the diffusion constant, D_b, of a Rh6G molecule in the bulk glycerol is calculated to be 1.06×10^{-12} m^2/s by using Eq. (4). The Stokes–Einstein equation gives the relation of the diffusion constant of a given molecule in a fluid continuum with the radius of the molecule (a) and the macroscopic viscosity of the fluid (η) dependent on the fluid temperature (T) as

$$D = \frac{kT}{6\pi\eta a} \tag{5}$$

where k is the Boltzmann constant. By using the glycerol temperature T of 307 K and D_b of 1.06×10^{-12} m^2/s, the effective hydrodynamic radius of a Rh6G moelcuels is obtained to be 5.0 nm, which is almost the same as the effective hydrodynamic radius of a Rh6G molecule in ethanol solution, in which Rh6G molecules are not aggregated [20]. This finding indicates that Rh6G molecules are dissolved separately in glycerol without any aggregation.

4.3. Fast diffusion of Rh6G aggregate at the air–glycerol interface

The molecular dynamics calculation has revealed that the interface region of glycerol, commonly defined as the region over which the density changes from 90% to 10% of the bulk density, is as narrow as ∼4 Å [3]. Let us consider a case that photon bursts from Rh6G aggregates are observed with adjusting the focal volume at the depth of 0 μm. A center of the focal volume is located in the interface region, but a part of it is extended in the bulk. Therefore, it is possible that the photon bursts come either from the aggregates traveling in the interface region or those in the bulk. If the photon bursts come from the aggregates traveling in the bulk, the widths of the photon bursts of the aggregates should be wider than those of Rh6G molecules dissolved molecularly in the bulk. However, the observed result is opposite to this conclusion. It follows that the characteristic time given by the cross-correlation analysis (see the discussion below) should be related to the two-dimensional translation motion of the aggregates on the interface. The correlation function of the two-dimensional translation motion is given by [21,22]

$$G(\tau) = G_s(0)\left(1 + \frac{\tau}{\tau_{D_s}}\right)^{-1} + \text{Const.} \quad (6)$$

where τ_{D_s} represents a two-dimensional diffusion time inside the probe volume on the air–glycerol interface, and $G_s(0)$ is the second power of the fluorescence intensity of the Rh6G aggregate on the air–glycerol interface. The term in Eq. (6) is contributed from the two-dimensional motion of the aggregates on the interface [19,20]. One obtains $\tau_{D_s} = 3.1 \pm 1.1$ ms by fitting of Eq. (6) to the cross-correlation shown in Fig. 5. By using Eq. (4), the diffusion constant (D_s) of the Rh6G aggregates on the air–glycerol interface was calculated to be 1.63×10^{-11} m^2/s, which is about 15 times larger than D_b.

It has been shown that the free-volume model is applicable to explanation of the high-pressure viscosity data of glycerol [2]. According to the model given by Doolittle [23] and Cohen and Turnbull [24], the pressure is written in terms of the viscosity of a liquid as:

$$\ln\left(\frac{\eta}{\eta_0}\right) = BV_\infty\left(\frac{1}{V - V_\infty} - \frac{1}{V_0 - V_\infty}\right) \quad (7)$$

where η_0 and V_0 are the viscosity and the volume of the liquid at the ambient pressure, respectively. The free volume of the liquid is represented by $V - V_\infty$, and the parameter, B, is related to the fragility of the liquid, which is described by the number of molecules moving cooperatively in order to facilitate transport of the liquid. A highly networked strong fluid (large B-value) requires cooperative displacement of more moieties than a molecular fragile liquid (small B-value). The viscosity, η, glycerol is sensitive to the change of its free volume V, because glycerol has a large B-value. On an air–glycerol interface, the hydrogen bonds in the glycerol are partially disrupted so that the fragility increases and the density decreases [3]. If the molecular picture for the bulk viscosity is applicable to estimate the viscosity of glycerol in the vicinity of the air–glycerol interface, the viscosity should be $\sim 10^{-3}$ times as large as that in the bulk glycerol on the assumption that the free volume of the glycerol interface is twice as large as that in bulk (see Eq. (7)).

As mentioned in the former subsections, Rh6G molecules with the average size of $\sim 7.5 \times 10^2$ are swiftly moving on the interface. The radius of a typical aggregate is estimated to be ∼17 nm by assuming that, (1) the aggregation is spherical and (2) the radius of a Rh6G molecule in the present aggregate is as large as that of a single Rh6G molecule composing a Rh6G J- or H-aggregate, namely 3.6 nm, while a Rh6G molecule in the outermost layer of the aggregate on the glycerol interface has the hydrodynamic radius of 5 nm. The radius is sufficiently larger than the thickness of the interface region so that the aggregate is considered to occupy a space across the border of the bulk and the interface, the interface region and the outside of the interface. The diffusion constant of the aggregate on the interface varies greatly with changing the volume fractions of the three different regions because of different viscosity constants in the bulk, the interface region and the outside. It was found that the viscosity constants could change by more than three orders of magnitude.

5. Summary

On the air–glycerol interface, Rh6G molecules are found to be assembled into aggregates having hydrodynamical radii of several tens nanometer. It was shown that the Rh6G aggregates diffuse two-dimensionally within the interface region, and the average diffusion constant is 15 times as large as the average diffusion constant of Rh6G molecules in the bulk glycerol. The average radius of the Rh6G aggregates is estimated to be larger than the thickness of the interface region if the aggregates are spherical, and hence the aggregates occupy a space across the bulk, the interface region and the outside of the interface. The solvation structure of the Rh6G aggregates in the vicinity of the interface region affects strongly on its diffusion dynamics because the viscosity constants of these three different regions differ by more than three orders of magnitude.

Acknowledgement

This research has been supported by the Special Cluster Research Project of the Genesis Research Institute Inc.

References

[1] L.J. Root, B.J. Berne, J. Chem. Phys. 107 (1997) 4350.
[2] R.L. Cook, H.E. King, Jr., C.A. Herbst, D.R. Herschbach, J. Chem. Phys. 100 (1994) 5178.

[3] I. Benjamin, M. Wilson, A. Pohorille, J. Chem. Phys. 100 (1994) 6500.
[4] M.E. Saecker, G.M. Nathanson, J. Chem. Phys. 99 (1993) 7056.
[5] O.N. Slyadneva, M.N. Slyadnev, A. Harata, T. Ogawa, Langmuir 17 (2001) 5329.
[6] K.B. Eisenthal, Chem. Rev. 96 (1996) 1343.
[7] V. Tsukanova, H. Lavoie, A. Harata, T. Ogawa, C. Salesse, J. Phys. Chem. B 106 (2002) 4203.
[8] X.-Y. Zheng, A. Harata, T. Ogawa, Chem. Phys. Lett. 316 (2000) 6.
[9] X.-Y. Zheng, A. Harata, T. Ogawa, Spectrochim. Acta, Part A 57 (2001) 315.
[10] M.D. Barnes, K.C. Ng, W.B. Whitten, J.M. Ramsey, Anal. Chem. 65 (1993) 2360.
[11] M.N. Slyadnev, T. Inoue, A. Harata, T. Ogawa, Colloids Surf. A: Physicochem. Eng. Aspects 164 (2000) 155.
[12] S. Nie, D.T. Chiu, R.N. Zare, Anal. Chem. 67 (1995) 2849.
[13] E.L. Elson, D. Magde, Biopolymers 13 (1974) 1.
[14] P.R. Bevington, D.K. Robinson, Data Reduction and Error Analysis for the Physical Sciences, second ed., McGraw-Hill Inc., 1992.
[15] χ^2 defined as $\chi^2 = \sum_i [h(x_i) - f(x_i)]/f(x_i)$ was obtained to be 13.9 responsible for the interface. The height distribution of the fluorescence photon counts related to fluorescence signals from the interface (see solid bars in Fig. 3) contains 17 data points, and the fitting parameters are two, A and λ. Therefore, the degrees of freedom (ν) turn out to be $\nu = 17 - 1 - 2 = 14$. As $\chi^2 = 13.9 < \chi^2_{0.05}(14) = 23.7$, we can accept the exponential function as a fitting function to the height distribution of the photon bursts at the 0.05 significant level. This argument is also true to the height distribution of the fluorescence photon counts responsible to the bulk glycerol.
[16] F.P. Schäfer (Ed.), Dye Lasers, Springer-Verlag, 1973.
[17] S. Nie, D.T. Chiu, R.N. Zare, Science 266 (1994) 1018.
[18] C. Bojarski, R. Bujko, P. Bojarski, Acta Phys. Pol. A 79 (1991) 471.
[19] E. Grabowska, J. Tyrzyk, C. Bojarski, Acta Phys. Pol. A57 (1980) 753.
[20] A.K. Chibisov, T.D. Slavnova, J. Photochem. 8 (1978) 285.
[21] D. Magde, E.L. Elson, W.W. Webb, Biopolymers 13 (1974) 29.
[22] S.R. Aragón, R. Pecora, J. Chem. Phys. 64 (1976) 1791.
[23] A.K. Doolittle, J. Appl. Phys. 22 (1951) 1471.
[24] M.H. Cohen, D. Turnbull, J. Chem. Phys. 31 (1959) 1164.